JOURNAL OF THE AMERICAN COLLEGE OF CARDIOLOGY
© 2015 BY THE AMERICAN COLLEGE OF CARDIOLOGY FOUNDATION
PUBLISHED BY ELSEVIER INC.
VOL. 66, NO. 8, 2015
ISSN 0735-1097/$36.00
http://dx.doi.org/10.1016/j.jacc.2015.06.1310

Valve-Related Hemodynamics Mediate Human Bicuspid Aortopathy

Insights From Wall Shear Stress Mapping

David G. Guzzardi, BSc,* Alex J. Barker, PhD,† Pim van Ooij, PhD,†‡ S. Chris Malaisrie, MD,§ Jyothy J. Puthumana, MD,‖ Darrell D. Belke, PhD,* Holly E.M. Mewhort, MD,* Daniyil A. Svystonyuk, BSc,* Sean Kang, BSc,* Subodh Verma, MD, PhD,¶ Jeremy Collins, MD,† James Carr, MD,† Robert O. Bonow, MD,‖ Michael Markl, PhD,†# James D. Thomas, MD,‖ Patrick M. McCarthy, MD,§# Paul W.M. Fedak, MD, PhD*§

ABSTRACT

BACKGROUND Suspected genetic causes for extracellular matrix (ECM) dysregulation in the ascending aorta in patients with bicuspid aortic valves (BAV) have influenced strategies and thresholds for surgical resection of BAV aortopathy. Using 4-dimensional (4D) flow cardiac magnetic resonance imaging (CMR), we have documented increased regional wall shear stress (WSS) in the ascending aorta of BAV patients.

OBJECTIVES This study assessed the relationship between WSS and regional aortic tissue remodeling in BAV patients to determine the influence of regional WSS on the expression of ECM dysregulation.

METHODS BAV patients (n = 20) undergoing ascending aortic resection underwent pre-operative 4D flow CMR to regionally map WSS. Paired aortic wall samples (i.e., within-patient samples obtained from regions of elevated and normal WSS) were collected and compared for medial elastin degeneration by histology and ECM regulation by protein expression.

RESULTS Regions of increased WSS showed greater medial elastin degradation compared to adjacent areas with normal WSS: decreased total elastin ($p = 0.01$) with thinner fibers ($p = 0.00007$) that were farther apart ($p = 0.001$). Multiplex protein analyses of ECM regulatory molecules revealed an increase in transforming growth factor β-1 ($p = 0.04$), matrix metalloproteinase (MMP)-1 ($p = 0.03$), MMP-2 ($p = 0.06$), MMP-3 ($p = 0.02$), and tissue inhibitor of metalloproteinase-1 ($p = 0.04$) in elevated WSS regions, indicating ECM dysregulation in regions of high WSS.

CONCLUSIONS Regions of increased WSS correspond with ECM dysregulation and elastic fiber degeneration in the ascending aorta of BAV patients, implicating valve-related hemodynamics as a contributing factor in the development of aortopathy. Further study to validate the use of 4D flow CMR as a noninvasive biomarker of disease progression and its ability to individualize resection strategies is warranted. (J Am Coll Cardiol 2015;66:892–900) © 2015 by the American College of Cardiology Foundation.

From the *Department of Cardiac Sciences, Libin Cardiovascular Institute of Alberta, University of Calgary, Calgary, Canada; †Department of Radiology, Feinberg School of Medicine, Northwestern University, Chicago, Illinois; ‡Department of Radiology, Academic Medical Center, Amsterdam, the Netherlands; §Division of Cardiac Surgery, Department of Surgery, Bluhm Cardiovascular Institute, Northwestern University, Chicago, Illinois; ‖Division of Cardiology, Department of Medicine, Bluhm Cardiovascular Institute, Northwestern University, Chicago, Illinois; ¶Division of Cardiac Surgery, Li Ka Shing Knowledge Institute of St. Michael's Hospital, University of Toronto, Toronto, Canada; and the #Department of Biomedical Engineering, McCormick School of Engineering, Northwestern University, Chicago, Illinois. Funded by Melman Bicuspid Aortic Valve Program, Bluhm Cardiovascular Institute (Dr. Fedak), American Heart Association grant 14POST20460151 (Dr. van Ooij), National Institutes of Health (NIH) grant K25HL119608 (Dr. Barker), and NIH grant R01HL115828 (Dr. Markl). Dr. Carr has a research agreement with Siemens. Dr. Thomas is a consultant for Abbott; and has received honoraria from Edwards Lifesciences, GE, and Abbott. All other authors have reported that they have no relationships relevant to the contents of this paper to disclose.
Listen to this manuscript's audio summary by *JACC* Editor-in-Chief Dr. Valentin Fuster.

Manuscript received April 16, 2015; revised manuscript received June 8, 2015, accepted June 12, 2015.

Bicuspid aortic valves (BAVs) are associated with an increased predisposition towards dilation of the ascending aorta that could increase the rates of aortic complications such as aortic dissection, rupture, and/or sudden death (1,2). Although several dilation patterns have been proposed (2), considerable debate remains as to whether they are due to an inherent aortic wall defect (i.e., genetic aortopathy) or are secondary to valve-related changes in regional hemodynamics and shear stress

SEE PAGE 901

(i.e., acquired etiology). A genetic etiology for BAV aortopathy is widely accepted and may prompt aggressive resection strategies to remove diseased tissues at risk of future complications (3,4). Increasingly, valve-related hemodynamics are believed to contribute to disease progression (5). Greater understanding of the pathophysiology of BAV aortopathy may facilitate improved surgical resection strategies, development of best practices and effective clinical guidelines, and in so doing, optimize clinical outcomes (6).

Flow-sensitive cardiac magnetic resonance imaging (CMR) with full volumetric coverage of the ascending aorta (4-dimensional [4D] flow CMR) can measure and visualize complex aortic 3-dimensional (3D) blood flow patterns, such as flow jets, vortices, and helical flow. Using 4D flow CMR, we previously observed that normally functioning BAVs are associated with disturbed flow patterns in the ascending aorta, with regional increases in wall shear stress (WSS) (7), a parameter known to be associated with vessel wall remodeling (8). We further established that the location of BAV cusp fusion is associated with different patterns of ascending aorta dilation (9). Recent studies have provided significant associative evidence that the pattern of cusp fusion corresponds with the expression of aortopathy (10,11), thus aligning with previous imaging findings implicating altered outflow patterns and the regional expression of elevated WSS with BAV morphology. To further investigate these findings, in this study, we measured aortic WSS by 4D flow CMR in healthy normal volunteers and BAV patients to detect non-physiological values, and for the first time, correlated valve-related changes in WSS to regional tissue architecture and remodeling in paired BAV aortic wall tissue samples.

METHODS

With internal review board approval and informed consent, 20 BAV patients referred for ascending aortic surgery were enrolled. Patients with previous ascending aortic surgery or evidence of other forms of connective tissue disease were excluded. Healthy age-matched controls (n = 10) with tricuspid aortic valves were enrolled to compute regionally resolved 95% confidence interval values for physiologically normal aortic WSS (12); these controls had no evidence of cardiovascular disease and did not undergo surgery. The degree of aortic stenosis was graded based on absolute systolic peak velocity by continuous-wave Doppler ultrasound (mild: 2 to 3 m/s; moderate/severe: ≥3 m/s), and aortic regurgitation was graded based on regurgitant fraction (mild: <30%; moderate/severe: ≥30%) (13).

Participants received pre-operative CMR at 1.5-T or 3-T (Magnetom Aera, Espree, Avanto, Skyra, Siemens Healthcare, Erlangen, Germany) to assess presence and significance of suspected BAV. 4D flow CMR provided complete volumetric coverage of the thoracic aorta for quantification of temporally resolved 3D blood flow velocities. Data were acquired during free breathing using respiratory and prospective electrocardiographic gating (14), with imaging parameters as described previously (12). Velocity encoding ranged from 150 to 400 cm/s based on the severity of valve stenosis. If the glomerular filtration rate was >30 ml/min, gadopentetate dimeglumine, gadofosveset trisodium, or gadobenate dimeglumine was administered intravenously, and the flip angle was set to 15°; otherwise, 7° was used. Patient-specific WSS heat maps of the BAV aorta were computed relative to a map of the population average for healthy age-matched controls as described in detail previously (12,15,16). WSS regions outside the healthy 95% confidence intervals were classified as abnormal. Intra-aortic regions of normal, depressed, and elevated WSS were mapped onto 3D visualizations of patient-specific aortas (**Figure 1**).

Aortic wall samples were collected as permitted by the extent of ascending aorta resection; surgeons were blinded to WSS heat maps. Samples were labeled according to pre-operative zonal designations relative to the position of the right pulmonary artery (zones 1, 2, and 3 correspond to regions proximal, adjacent, and distal to the right pulmonary artery, respectively) (**Figure 1**), and according to circumferential location (greater curvature, lesser curvature, anterior or posterior wall). Tissue samples were divided in 2 for histology and protein analysis, flash-frozen in optimal cutting temperature freezing compound (VWR International, Radnor, Pennsylvania)

ABBREVIATIONS AND ACRONYMS

3D = 3-dimensional
4D = 4-dimensional
BAV = bicuspid aortic valve
CMR = cardiac magnetic resonance imaging
ECM = extracellular matrix
IQR = interquartile range
MMP = matrix metalloproteinase
TGF = transforming growth factor
TIMP = tissue inhibitor of matrix metalloproteinase
WSS = wall shear stress

FIGURE 1 BAV Aortas: WSS Heat Maps and Elastin Fiber Staining

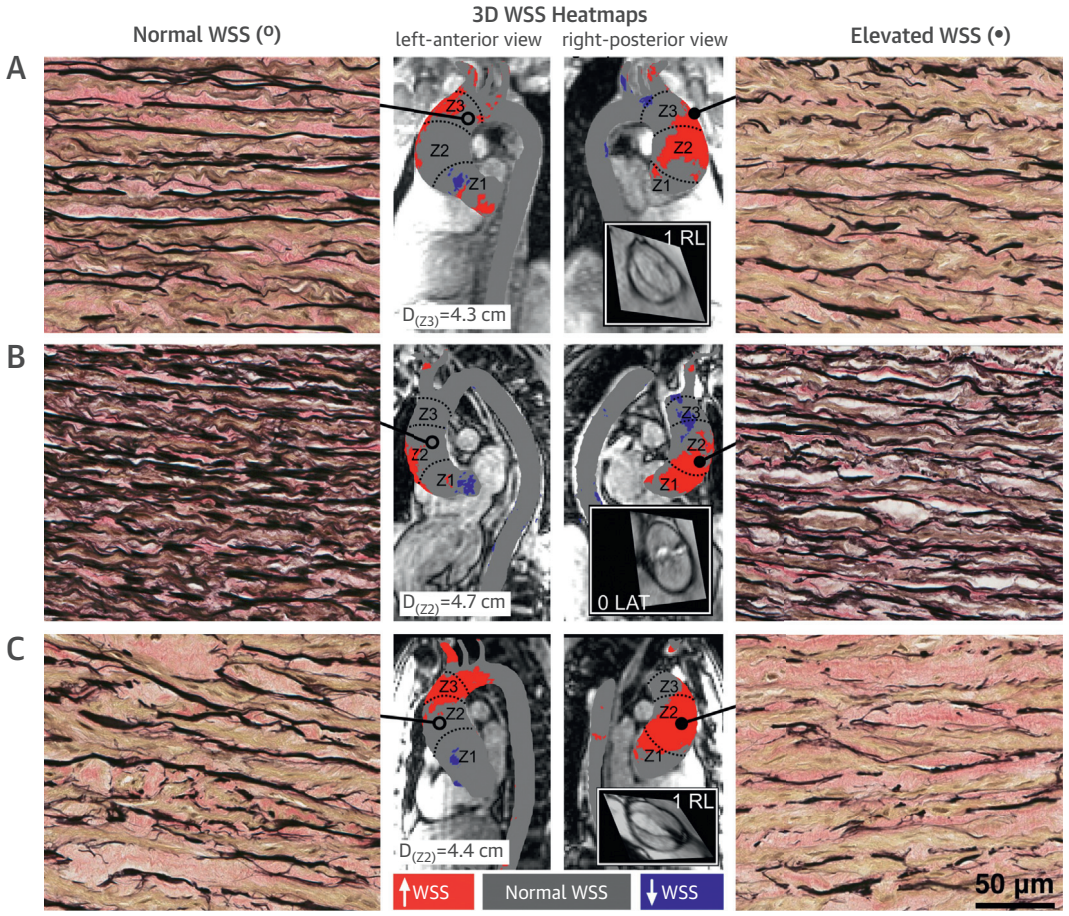

Aortic wall (**A, B, and C** denote 3 different bicuspid aortic valve [BAV] aortas) from regions of high wall shear stress (WSS) **(right panels; closed circles)** had fewer elastin fibers **(black)** that were thinner and farther apart compared with regions with normal WSS **(left panels; open circles)** in the same human aortas (40× magnification). Samples were collected from zone 1, 2, or 3, and from either the greater curvature, lesser curvature, or anterior or posterior walls; accompanying diameters for tissue collection sites are shown. **Grey** denotes normal WSS within the 95% confidence interval compared with a healthy tricuspid aortic valve population; **red and purple** denote elevated and depressed WSS, respectively. **Insets** show steady-state free precession images of the aortic valve and Sievers valve phenotype. 3D = 3-dimensional.

and liquid nitrogen within 15 min of resection, and then stored at −80°C until use. Paired samples of each patient's aorta from regions of normal and elevated WSS were compared.

Tissue designated for histology was thawed, sectioned circumferentially, and then fixed in 10% buffered neutral formalin (VWR International) for a maximum of 1 week and paraffin-embedded. Sections of 6 μm were mounted for Verhoeff-Van Gieson staining of medial elastin fibers. Chromatic analysis of elastin abundance was performed (Aperio ePathology, Leica Biosystems, Buffalo Grove, Illinois). Total elastin content was computed as the mean percent area of elastin staining relative to the total area analyzed of 6 representative fields of view (40× magnification) as selected by blinded observer. Distance between intact elastin fibers and their thicknesses were measured (ImageScope Viewing Software, Leica Biosystems) by blinded observer with a mean value computed for each sample taken from an average of 131 measurements per circumferentially sectioned slide (as described by Bauer et al. [17]).

Tissue designated for protein quantification was homogenized in 20 mmol/l Tris-HCl buffer (pH 7.5, 0.5% Tween 20, 150 mmol/l NaCl, and Roche

TABLE 1 Patient Characteristics in BAV Study Population (N = 20)

Age, yrs	48 ± 15
Female	2 (10)
BAV classification	
Type 0, lateral	2 (10)
Type 1, RN	1 (5)
Type 1, RL	12 (60)
Type 2, RL/RN	5 (25)
Aortic diameter, cm	
Sinus of Valsalva	4.4 ± 0.5 (range 3.7-5.7)
Mid ascending aorta	4.7 ± 0.6 (range 3.6-6.3)
Aortic valve function	
No AS, moderate/severe AR	5 (25)
Mild AS, moderate/severe AR	1 (5)
Moderate/severe AS, no AR	5 (25)
Moderate/severe AS, mild AR	3 (15)
Moderate/severe AS, moderate/severe AR	6 (30)
Hypertension	7 (35)
Surgical procedure: aortic valve	
Repair	1 (5)
Replacement	19 (95)
AVR	4 (20)
Bentall	14 (70)
Ross	1 (5)
Surgical procedure: AsAo	
AsAo replacement	20 (100)
Root replacement	16 (80)
Hemi-arch	8 (40)

Values are mean ± SD or n (%).

AR = aortic regurgitation; AS = aortic stenosis; AsAo = ascending aorta; AVR = aortic valve replacement; BAV = bicuspid aortic valve; RL = right-left coronary cusp fusion; RN = right coronary–noncoronary cusp fusion.

complete protease inhibitor 1:100) and centrifuged at 10,000 *g* for 10 min at 4°C. Supernatant containing 1.0 μg of protein was assayed in duplicate for concentration of transforming growth factor (TGF)-β-1, matrix metalloproteinases (MMPs), and tissue inhibitors of MMPs (TIMP) using the multiplex fluorescent bead assay (Eve Technologies, Calgary, Alberta, Canada).

STATISTICAL ANALYSIS. All group data are presented as mean ± SD if normally distributed or as median (interquartile range [IQR]) if non-normally distributed. Normality was assessed using the Shapiro-Wilk test. Normally and non-normally distributed data were compared using a paired Student *t* test or the Wilcoxon signed rank test, respectively (both 2-tailed). Cohort-averages between 2 groups were compared using the Student *t* test when normally distributed or the Mann-Whitney test when non-normally distributed. Statistical analyses were performed using GraphPad Prism 6.0 (GraphPad Software, La Jolla, California), with $p < 0.05$ considered statistically significant.

RESULTS

Patient demographics are summarized in Table 1. Healthy controls were used to define physiologically normal WSS values and were age-matched to BAV patients (50 ± 14 years vs. 48 ± 15 years, respectively; p = 0.83). BAV patients were predominantly male with type 1 fusion of the right and left coronary cusps. Surgery was primarily indicated for BAV dysfunction; all patients had moderate/severe stenosis or regurgitation. Mean aortic diameter was 4.4 ± 0.5 cm at the sinus of Valsalva and 4.7 ± 0.6 cm for the ascending aorta. Most patients underwent aortic valve replacement (1 patient underwent BAV repair). All patients had ascending aortic resection, with most requiring concomitant root replacement and a few undergoing hemiarch resection using deep hypothermic circulatory arrest. Tissue corresponding to regions of normal and elevated WSS were primarily collected from zone 2 of the BAV aorta and from the anterior wall and greater curvature, respectively. Samples collected from patients are summarized in Online Table.

We quantified the total elastin content and architecture by histology image analysis. Aortic wall from regions of normal and elevated WSS demonstrated significantly decreased elastin content and architecture consistent with aortopathy (Figures 1A to 1C). Aortic wall exposed to elevated WSS showed reduced elastin abundance compared with aortic wall subjected to normal WSS within the same aorta (p = 0.01) (Figure 2A). Similarly, the cohort-averaged percent area of elastin was significantly decreased in regions of elevated WSS among BAV aortas (36.61 ± 16.87% vs. 49.12 ± 16.53%; p = 0.04) (Figure 2B). Compared with aortic wall subjected to normal WSS, regions of elevated WSS had elastin fibers that were significantly thinner among patient pairs (p = 0.00007) (Figure 2C). The absolute mean thickness of elastin fibers also was significantly decreased in regions of elevated WSS compared with regions of normal WSS (2.72 ± 0.40 μm vs. 3.25 ± 0.27 μm; p = 0.00002) (Figure 2D). The median distance between elastin fibers was significantly greater in regions of elevated WSS compared to normal WSS (p = 0.001) (Figure 2E). Similarly, cohort-averaged median distance between elastin fibers was significantly increased in aortic wall subjected to elevated WSS (28.34 μm [IQR: 22.03 to 36.32 μm] vs. 20.39 μm [IQR: 18.35 to 24.43 μm]; p = 0.01) (Figure 2F).

FIGURE 2 Metrics of Elastin Fiber Architecture

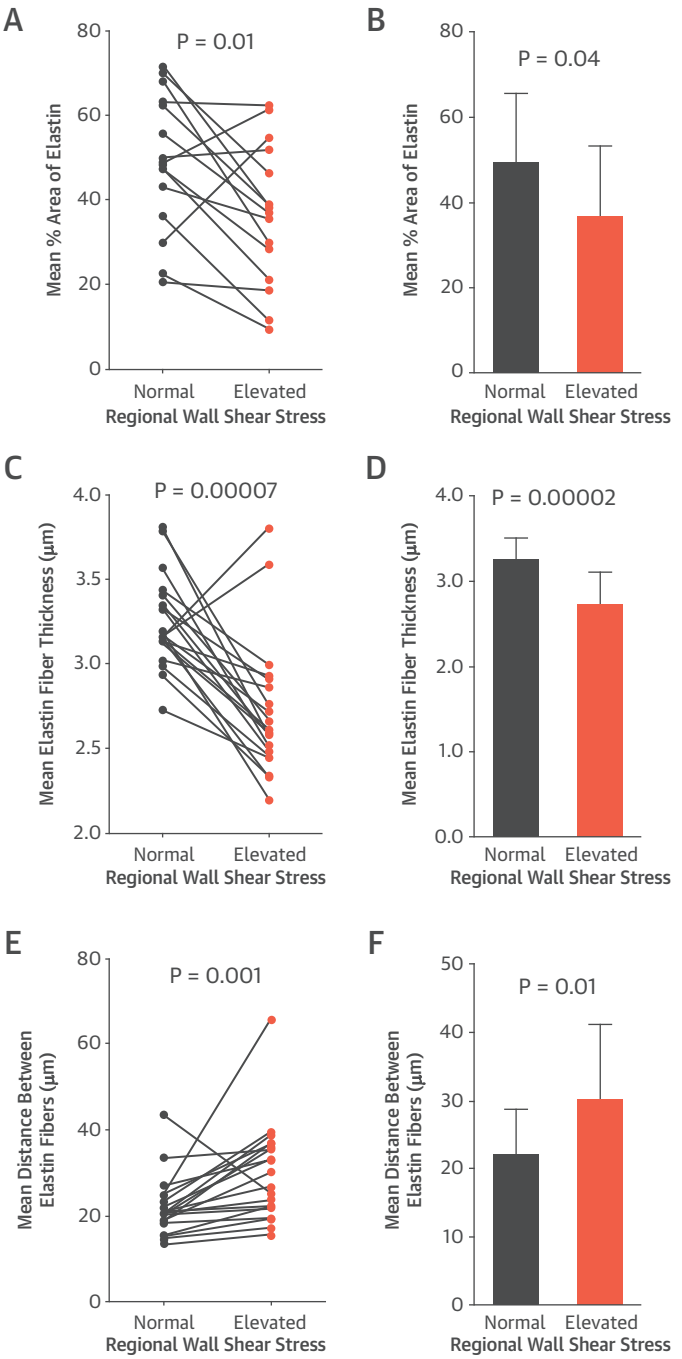

Elastin fiber characteristics from Verhoeff-Van Gieson elastin staining for patient pairs **(A, C, and E)** and cumulative group means **(B, D, and F)** for aortic wall subjected to normal and elevated WSS are shown. Total percent area of elastin staining was decreased in regions of elevated WSS compared to normal WSS **(A and B)**, and remaining fibers were thinner **(C and D)**. Greater distances between intact adjacent elastin fibers were observed in regions of elevated WSS **(E and F)**. Abbreviations as in Figure 1.

Regions of elevated WSS had significantly higher concentrations of TGFβ-1 protein ($p = 0.04$) (Figure 3) compared with paired regions of normal WSS in the same aortas.

Aortic wall subjected to normal and elevated WSS within each patient's aorta were profiled for MMP and TIMP protein concentrations (Table 2). The absolute levels of MMP and TIMP protein expression in the samples were highly variable. MMP-2 and TIMP-2 were the most highly expressed MMP and TIMP in the aorta. Compared with regions of normal WSS, aortic wall exposed to elevated WSS demonstrated significantly increased relative concentrations of MMP-1 ($p = 0.03$), MMP-3 ($p = 0.02$), and TIMP-1 ($p = 0.04$), and there was a trend ($p = 0.06$) for increased concentrations of MMP-2.

DISCUSSION

BAV is an inheritable disorder, and a genetic theory for the associated aortopathy is widely held, positing that the aorta has an inherent genetic weakness and is prone to dilation and rupture from an underlying dysregulation of extracellular matrix (ECM) in the aortic medial layer (1,5). This perspective has encouraged more aggressive approaches towards aortic resection using strategies similar to those applied in patients with proven genetic aortopathies, such as Marfan syndrome. Recently, we and others have shown that valve-related hemodynamics may play an important role in disease progression, where altered flow in the aorta is consistent with patterns of aortic dilation (9-11,18,19). Recognizing that hemodynamics may be altered in different regions of the ascending aorta, regional differences have been documented in key ECM proteins and cell phenotypic expressions, focused primarily on the convexity versus the concavity of the BAV aorta (20,21). These translational tissue studies suggest that valve-related hemodynamics may influence disease progression.

There is mounting evidence that both theories may coexist (5,22). Valve-related hemodynamics may exacerbate disease progression in genetically susceptible aortas (6). Given the absence of data showing a mechanistic link between cusp fusion patterns, altered aortic flow, and expression of disease, considerable debate surrounds the role of hemodynamics in mediating BAV aortopathy (5). Recently, using 4D flow CMR, we observed that even normally functioning BAVs are associated with disturbed ascending aortic flow and regional WSS increases, beyond the hemodynamic derangements accounted for by measures of stenosis and regurgitation (7). We further

FIGURE 3 TGFβ-1 Concentrations in Regions of Normal and Elevated WSS

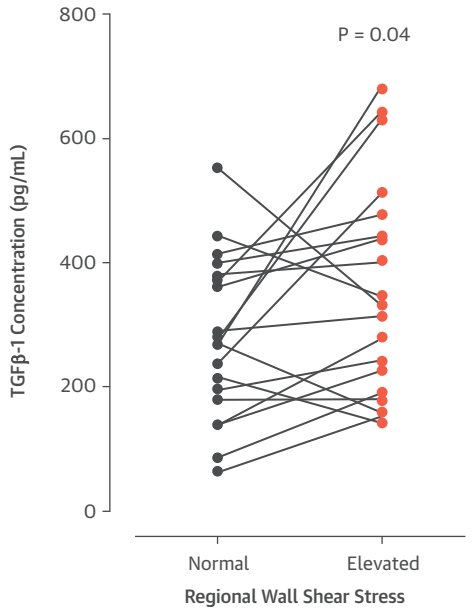

Absolute transforming growth factor β-1 (TGFβ-1) concentrations were greater in aortic wall regions of elevated compared with normal wall sheer stress (WSS). **Solid lines** denote group means, and p value represents analysis between paired patient samples (normal and elevated WSS).

established that the location of BAV cusp fusion was associated with different patterns of ascending aortic dilation (9), suggesting that valve-related hemodynamics may influence the expression of BAV aortopathy.

Despite well-documented changes of WSS in BAV patients, its role in the underlying aortopathy is unclear. In the current study, distinct regions of increased WSS were uniformly observed in BAV patients despite varied cusp fusion patterns and types or degrees of valve dysfunction. The significant relationship between WSS derived from 4D flow CMR and regional aortic tissue remodeling provides evidence, for the first time, of the role of valve-related hemodynamics in BAV aortopathy (**Central Illustration**).

WSS CORRESPONDS TO CHANGES RELATED TO AORTOPATHY. To validate the influence of regional WSS on tissue remodeling, we compared the medial matrix architecture between areas of high and normal WSS within each BAV aorta. This analysis is advantageous because each patient serves as his or her own control. Degeneration of the aortic media, particularly its elastic laminae, is the *sine qua non* of BAV aortopathy, with a hallmark of elastic fiber fragmentation (23). Bauer et al. (17) also observed medial elastin degeneration characteristic of BAV aortopathy, documenting thinner elastic laminae and increased distances between laminae. In patients with BAV stenosis undergoing aortic valve replacement, Girdauskas et al. (24) documented qualitative differences in aortic histology at the level of aortotomy with different systolic transvalvular flow patterns.

We observed disrupted medial elastin fiber architecture in the aortic wall of our patient cohort, consistent with BAV aortopathy, coupled with the novel finding that elastin fiber fragmentation and architectural derangement was significantly increased in areas of high versus normal WSS within the same aortas. Areas of normal WSS also had evidence of medial matrix degradation consistent with BAV aortopathy, although less severe than corresponding areas of high WSS. Given that histological abnormalities are diffuse within the BAV aorta and our study population had relatively mild levels of aortic dilation (most <5.0 cm), the increased elastin degradation observed in the areas of high WSS relative to adjacent areas with normal WSS is a striking observation that provides strong evidence implicating valve-related hemodynamics in medial matrix degradation in BAV aortopathy.

TGFβ is strongly implicated in the mechanotransduction of WSS upstream of flow-induced vascular remodeling (25). In animal models of human aortopathy, TGFβ signaling is implicated in vascular disease and progression as a critical mediator of aortopathy (26). Forte and colleagues (20) showed that TGFβ and TGFβ receptor-2 are increased in BAV aorta, suggesting a role for TGFβ in mediating disease. In this study, we provide novel data linking aortic TGFβ protein expression to local increases in WSS, with ascending aortic TGFβ concentration significantly elevated in regions of high aortic WSS compared with adjacent regions with normal WSS. These data strongly implicate WSS as contributing to TGFβ expression in the BAV aorta.

MMPs can directly degrade elastic ECM components. Supporting a mechanistic role for valve-related hemodynamics in MMP expression, Ikonomidis et al. (27) showed altered MMP profiles stratified by cusp fusion pattern in the BAV aorta. Although many MMPs are expressed in the aorta, MMP-2 is highly implicated in aortic aneurysms and elastic matrix degeneration of remodeled arteries (28). Animal models provide proof of concept for WSS as a trigger for aortic wall MMP activation. For example, flow-mediated induction of MMP-2 expression was

TABLE 2 Absolute MMP and TIMP Concentrations in BAV Aortas

	Median Concentration (pg/ml)	IQR (pg/ml)	Range (pg/ml)	p Value
MMP-1*				
Elevated WSS	11.04	5.8–20.5	2.4–148.2	0.027
Normal WSS	8.84	3.5–14.7	1.3–19.3	
MMP-2				
Elevated WSS	8,093.00	5,062.0–13,691.0	293.3–185,897.0	0.064
Normal WSS	6,060.00	2,621.0–12,910.0	197.1–119,902.0	
MMP-3				
Elevated WSS	85.28	51.6–162.8	29.2–485.1	0.019
Normal WSS	58.46	43.4–115.9	6.8–363.8	
MMP-7*				
Elevated WSS	75.3†	54.2‡	8.5–165.6	0.653
Normal WSS	69.3†	72.7‡	0.0–235.3	
MMP-8				
Elevated WSS	2,596.0	778.4–6,258.0	22.4–22,744.0	0.294
Normal WSS	3,594.0	1,754.0–7,706.0	404.5–37,267.0	
MMP-9				
Elevated WSS	4,806.0	2,377.0–19,356.0	479.6–74,046.0	0.596
Normal WSS	6,581.0	3,582.0–11,796.0	1,588.0–12,6759.0	
MMP-10*				
Elevated WSS	14.2	7.2–17.7	1.8–45.9	0.229
Normal WSS	10.5	8.1–13.1	0.7–36.1	
TIMP-1				
Elevated WSS	21,442.0	11,499.0–36,679.0	4,022.0–151,540.0	0.040
Normal WSS	14,546.0	8,485.0–19,629.0	4,136.0–14,9919.0	
TIMP-2				
Elevated WSS	24,931.0	15,476.0–48,537.0	1,0399.0–171,363.0	0.756
Normal WSS	21,721.0	14,892.0–40,513.0	6,384.0–336,986.0	
TIMP-3				
Elevated WSS	4,138.0†	2,991.0‡	0.0–11,961.0	0.079
Normal WSS	3,272.0†	2,794.0‡	0.0–9,862.0	
TIMP-4				
Elevated WSS	92.2	47.9–148.0	14.7–1,173.0	0.165
Normal WSS	79.0	57.7–128.9	1.9–840.1	

*Number of samples outside range of detection: MMP-1 = 7, MMP-7 = 10, and MMP-10 = 2. Concentrations are reported as median [IQR] when nonnormally distributed or mean (†) ± SD (‡) when normally distributed. p Values denote paired analyses between regions of normal and elevated WSS in each BAV aorta.

IQR = interquartile range; MMP = matrix metalloproteinase; TIMP = tissue inhibitor of matrix metalloproteinase; WSS = wall shear stress; other abbreviations as in Table 1.

demonstrated in rabbit carotid arteries in association with medial matrix degeneration and vessel dilation (29). Furthermore, Atkins et al. (30) modeled BAV-related elevated WSS in an ex vivo porcine aorta system, and found increased MMP-2 expression and activity. We previously reported evidence of MMP-2 elevations in the BAV aorta (31). The cumulative evidence by meta-analysis of all such studies confirms that MMP-2 is consistently elevated in human BAV aortopathy (32).

In the current study, we observed that aortic wall MMP-2 was the most highly expressed MMP in the BAV aorta, with a trend ($p = 0.06$) for greater expression in areas of high WSS as compared to adjacent areas with normal WSS in the same patients, and with significant increases in MMP-3 in the same areas. Importantly, the elevated levels of MMP-2, MMP-3, and TGFβ areas of increased WSS were associated with fragmented medial elastin fibers. This observation also strongly implicates WSS in mediating BAV aortic disease progression. In addition to a direct role in degrading elastic tissue, it is noteworthy that MMP-2 and MMP-3 can activate latent TGFβ and increase its activity. These factors may work synergistically to induce medial matrix remodeling.

The observed TIMP changes are complex, and the substantial variability between patients and regions studied suggests that the regulatory control of TIMP expression is less influenced by WSS than specific MMPs and TGFβ. TIMP-1 levels were increased in areas of high WSS, but no significant difference was observed between groups with respect to other TIMP species. The lack of increased compensatory TIMP-2 expression in areas of high WSS may result in heightened MMP-2 activity. Further study is required to better define and understand the influence of specific MMPs and TIMPs in BAV aortopathy and their expression and activities with respect to valve-related hemodynamics.

STUDY LIMITATIONS. In our study, 4D flow CMR was used as a research tool to obtain WSS maps in individual patient aortas to better understand whether blood flow patterns play a role in the expression of BAV aortopathy. Given the spatial and temporal resolution of 4D flow CMR, underestimation of WSS is known to occur (7); however, relative WSS values (i.e., high/low WSS) are retained between subjects when consistent imaging parameters are employed. Here, we used similar parameters to those of a prior study that demonstrated the robustness of WSS measurements (33). Additionally, same-patient samples ensured that the relative WSS measurements were obtained in the same subject and same exam. Therefore, resolution was not deemed a significant factor for the study protocol to detect elevated WSS. Although the concentrations of specific proteins of interest were examined, further studies should investigate TGFβ and MMP-2 activities and other associated factors such as shifts in cell phenotype that may also mediate matrix remodeling. Additional comparison to patients with tricuspid valves and dilated aortas with areas of increased WSS should also be explored.

CENTRAL ILLUSTRATION **4D Flow CMR and BAV Aortopathy**

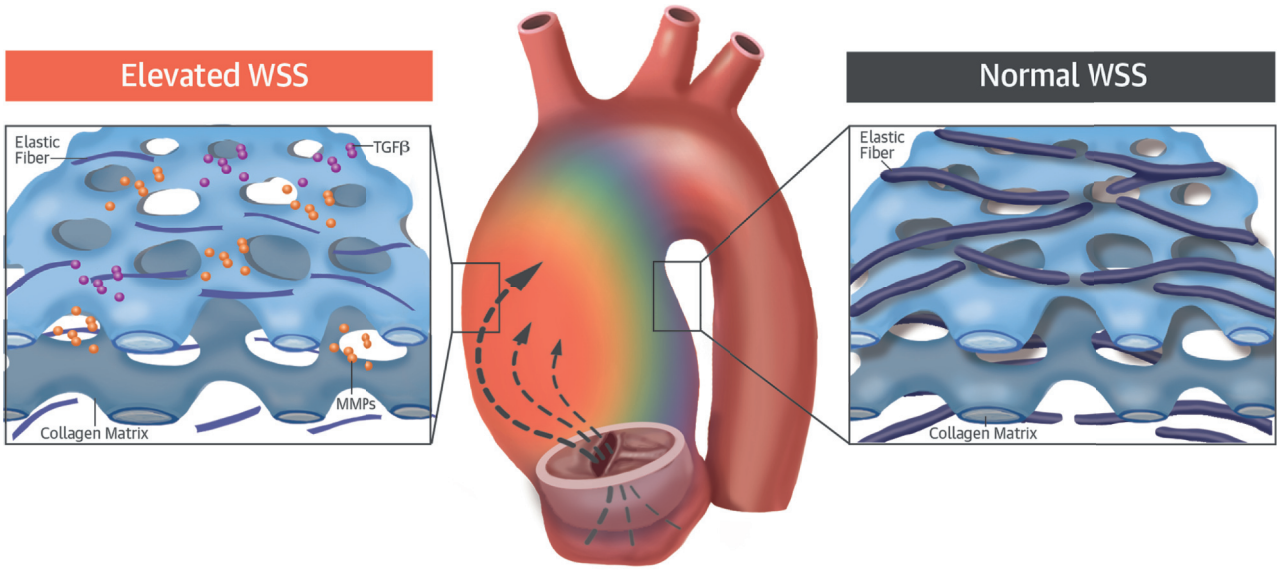

Guzzardi, D.G. et al. J Am Coll Cardiol. 2015; 66(8):892-900.

Using 4-dimensional flow cardiac magnetic resonance imaging (4D flow CMR), we assessed the relation between wall shear stress (WSS) and regional aortic tissue remodeling in bicuspid aortic valve (BAV) patients. Elevated aortic WSS generated by aberrant flow from cusp fusion corresponded to more severe extracellular matrix (ECM) dysregulation than adjacent regions of normal WSS in the same patient's aorta. Characteristic medial degeneration was observed throughout the aorta, but elastic fiber degeneration was more severe in regions of elevated WSS (less elastin, thinner fibers, and greater distances between laminae), where higher concentrations of mediators of ECM dysregulation (matrix metalloproteinase [MMP] and transforming growth factor β [TGFβ]) are also observed. These data implicate valve-related hemodynamics as a contributing factor to BAV aortopathy.

CONCLUSIONS

Regions of increased WSS correspond with ECM dysregulation and elastic fiber degeneration in the ascending aorta of BAV patients, implicating valve-related hemodynamics as a mediator of aortopathy. WSS as assessed by 4D flow CMR may serve as a noninvasive biomarker of regional aortic disease in patients with BAV aortopathy (deemed sufficiently severe to warrant operative intervention). Its utility in prediction of disease progression, particularly in earlier and less severe BAV aortopathy, awaits careful study, as does the efficacy of a targeted surgical approach incorporating regional aortic WSS.

ACKNOWLEDGMENTS The authors gratefully acknowledge the recruitment and organizational efforts of Colleen Clennon (Northwestern University), the staff of Northwestern's Center for Translational Imaging, Drs. Amy Bromley (University of Calgary) and Yong-Xiang Chen (University of Calgary) for their histological expertise, and Thomas Kryton for histological database management (University of Calgary).

REPRINT REQUESTS AND CORRESPONDENCE: Dr. Paul W.M. Fedak, Department of Cardiac Sciences, University of Calgary, Room 880, 1403-29 Street NW, Calgary, Alberta T2N 2T9, Canada. E-mail: paul.fedak@gmail.com.

PERSPECTIVES

COMPETENCY IN MEDICAL KNOWLEDGE: Measurements made using 4D flow CMR suggest that valve-related hemodynamics contribute to the development of aortopathy in patients with BAV.

TRANSLATIONAL OUTLOOK: Validation studies are needed to confirm the utility of 4D flow CMR as a noninvasive marker of disease progression, predictor of aortic dissection or rupture, and guide to the extent of surgical resection based on detailed measurements of regional aortic wall shear stress.

REFERENCES

1. Fedak PW, Verma S, David TE, et al. Clinical and pathophysiological implications of a bicuspid aortic valve. Circulation 2002;106:900–4.

2. Verma S, Siu SC. Aortic dilatation in patients with bicuspid aortic valve. N Engl J Med 2014;370:1920–9.

3. Verma S, Yanagawa B, Kalra S, et al. Knowledge, attitudes, and practice patterns in surgical management of bicuspid aortopathy: a survey of 100 cardiac surgeons. J Thorac Cardiovasc Surg 2013;146:1033–40.e4.

4. Rinewalt D, McCarthy PM, Malaisrie SC, et al. Effect of aortic aneurysm replacement on outcomes after bicuspid aortic valve surgery: Validation of contemporary guidelines. J Thorac Cardiovasc Surg 2014;148:2060–9.

5. Girdauskas E, Borger MA, Secknus MA, et al. Is aortopathy in bicuspid aortic valve disease a congenital defect or a result of abnormal hemodynamics? A critical reappraisal of a one-sided argument. Eur J Cardiothorac Surg 2011;39:809–14.

6. Della Corte A, Body SC, Booher AM, et al. Surgical treatment of bicuspid aortic valve disease: knowledge gaps and research perspectives. J Thorac Cardiovasc Surg 2014;147:1749–57, 1757.e1.

7. Barker AJ, Markl M, Burk J, et al. Bicuspid aortic valve is associated with altered wall shear stress in the ascending aorta. Circ Cardiovasc Imaging 2012;5:457–66.

8. Lehoux S, Tedgui A. Cellular mechanics and gene expression in blood vessels. J Biomech 2003;36:631–43.

9. Mahadevia R, Barker AJ, Schnell S, et al. Bicuspid aortic cusp fusion morphology alters aortic three-dimensional outflow patterns, wall shear stress, and expression of aortopathy. Circulation 2014;129:673–82.

10. Kang JW, Song HG, Yang DH, et al. Association between bicuspid aortic valve phenotype and patterns of valvular dysfunction and bicuspid aortopathy: comprehensive evaluation using MDCT and echocardiography. J Am Coll Cardiol Img 2013;6:150–61.

11. Della Corte A, Bancone C, Dialetto G, et al. Towards an individualized approach to bicuspid aortopathy: different valve types have unique determinants of aortic dilatation. Eur J Cardiothorac Surg 2014;45:e118–24; discussion e124.

12. van Ooij P, Potters WV, Collins J, et al. Characterization of abnormal wall shear stress using 4D flow MRI in human bicuspid aortopathy. Ann Biomed Eng 2015;43:1385–97.

13. Nishimura RA, Otto CM, Bonow RO, et al. 2014 AHA/ACC guideline for the management of patients with valvular heart disease: a report of the American College of Cardiology/American Heart Association Task Force on Practice Guidelines. J Am Coll Cardiol 2014;63:e57–185.

14. Markl M, Harloff A, Bley TA, et al. Time-resolved 3D MR velocity mapping at 3T: improved navigator-gated assessment of vascular anatomy and blood flow. J Magn Reson Imaging 2007;25:824–31.

15. van Ooij P, Potters WV, Nederveen AJ, et al. A methodology to detect abnormal relative wall shear stress on the full surface of the thoracic aorta using four-dimensional flow MRI. Magn Reson Med 2015;73:1216–27.

16. Potters WV, van Ooij P, Marquering H, van Bavel E, Nederveen AJ. Volumetric arterial wall shear stress calculation based on cine contrast MRI. J Magn Reson Imaging 2015;41:505–16.

17. Bauer M, Pasic M, Meyer R, et al. Morphometric analysis of aortic media in patients with bicuspid and tricuspid aortic valve. Ann Thorac Surg 2002;74:58–62.

18. Bissell MM, Hess AT, Biasiolli L, et al. Aortic dilation in bicuspid aortic valve disease: flow pattern is a major contributor and differs with valve fusion type. Circ Cardiovasc Imaging 2013;6:499–507.

19. Hope MD, Hope TA, Meadows AK, et al. Bicuspid aortic valve: four-dimensional MR evaluation of ascending aortic systolic flow patterns. Radiology 2010;255:53–61.

20. Forte A, Della Corte A, Grossi M, et al. Early cell changes and TGFbeta pathway alterations in the aortopathy associated with bicuspid aortic valve stenosis. Clin Sci 2013;124:97–108.

21. Cotrufo M, Della Corte A, De Santo LS, et al. Different patterns of extracellular matrix protein expression in the convexity and the concavity of the dilated aorta with bicuspid aortic valve: preliminary results. J Thorac Cardiovasc Surg 2005;130:504–11.

22. Della Corte A. The conundrum of aortic dissection in patients with bicuspid aortic valve: the tissue, the mechanics and the mathematics. Eur J Cardiothorac Surg 2015;48:150–1.

23. de Sa M, Moshkovitz Y, Butany J, David TE. Histologic abnormalities of the ascending aorta and pulmonary trunk in patients with bicuspid aortic valve disease: clinical relevance to the Ross procedure. J Thorac Cardiovasc Surg 1999;118:588–94.

24. Girdauskas E, Rouman M, Disha K, et al. Correlation between systolic transvalvular flow and proximal aortic wall changes in bicuspid aortic valve stenosis. Eur J Cardiothorac Surg 2014;46:234–9; discussion 239.

25. Ohno M, Cooke JP, Dzau VJ, Gibbons GH. Fluid shear stress induces endothelial transforming growth factor beta-1 transcription and production. Modulation by potassium channel blockade. J Clin Invest 1995;95:1363–9.

26. Holm TM, Habashi JP, Doyle JJ, et al. Noncanonical TGFbeta signaling contributes to aortic aneurysm progression in Marfan syndrome mice. Science 2011;332:358–61.

27. Ikonomidis JS, Ruddy JM, Benton SM Jr., et al. Aortic dilatation with bicuspid aortic valves: cusp fusion correlates to matrix metalloproteinases and inhibitors. Ann Thorac Surg 2012;93:457–63.

28. Chung AW, Au Yeung K, Sandor GG, et al. Loss of elastic fiber integrity and reduction of vascular smooth muscle contraction resulting from the upregulated activities of matrix metalloproteinase-2 and -9 in the thoracic aortic aneurysm in Marfan syndrome. Circ Res 2007;101:512–22.

29. Tronc F, Mallat Z, Lehoux S, et al. Role of matrix metalloproteinases in blood flow-induced arterial enlargement: interaction with NO. Arterioscler Thromb Vasc Biol 2000;20:E120–6.

30. Atkins SK, Cao K, Rajamannan NM, Sucosky P. Bicuspid aortic valve hemodynamics induces abnormal medial remodeling in the convexity of porcine ascending aortas. Biomech Model Mechan 2014;13:1209–25.

31. Fedak PW, de Sa MP, Verma S, et al. Vascular matrix remodeling in patients with bicuspid aortic valve malformations: implications for aortic dilatation. J Thorac Cardiovasc Surg 2003;126:797–806.

32. Rabkin SW. Differential expression of MMP-2, MMP-9 and TIMP proteins in thoracic aortic aneurysm: comparison with and without bicuspid aortic valve: a meta-analysis. VASA 2014;43:433–42.

33. Markl M, Wallis W, Harloff A. Reproducibility of flow and wall shear stress analysis using flow-sensitive four-dimensional MRI. J Magn Res Imaging 2011;33:988–94.

KEY WORDS aneurysm, imaging, remodeling

APPENDIX For a supplemental table, please see the online version of this article.